HYBRID ACTIVE/PASSIVE CONTROL OF SOUND RADIATION FROM PANELS WITH CONSTRAINED LAYER DAMPING AND MODEL PREDICTIVE FEEDBACK CONTROL

Randolph H. Cabell and Gary P. Gibbs
Structural Acoustics Branch
NASA Langley Research Center
Hampton, VA 23681

INTRODUCTION

There has been considerable interest over the past several years in applying feedback control methods to problems of structural acoustics. One problem of particular interest is the control of sound radiation from aircraft panels excited on one side by a turbulent boundary layer (TBL). TBL excitation appears as many uncorrelated sources acting on the panel, which makes it difficult to find a single reference signal that is coherent with the excitation. Feedback methods have no need for a reference signal, and are thus suited to this problem. Some important considerations for the structural acoustics problem include the fact that the required controller bandwidth can easily extend to several hundred Hertz, so a digital controller would have to operate at a few kilohertz. In addition, aircraft panel structures have a reasonably high modal density over this frequency range. A model based controller must therefore handle the modally dense system, or have some way to reduce the bandwidth of the problem. Further complicating the problem is the fact that the stiffness and dynamic properties of an aircraft panel can vary considerably during flight due to altitude changes resulting in significant resonant frequency shifts.

These considerations make the tradeoff between robustness to changes in the system being controlled and controller performance especially important. Recent papers concerning the design and implementation of robust controllers for structural acoustic problems highlight the need to consider both performance and robustness when designing the controller [1, 2]. While robust control methods such as H_∞ can be used to balance performance and robustness [3], their implementation is not easy and requires assumptions about the types of uncertainties in the plant being controlled. Achieving a useful controller design may require many tradeoff studies of different types of parametric uncertainties in the system [1].

Another approach to achieving robustness to plant changes is to make the controller adaptive. For example, a mathematical model of the plant could be periodically updated as the plant changes, and the feedback gains recomputed from the updated model [4]. To be practical, this approach requires a simple plant model that can be updated quickly with reasonable computational requirements. A recent paper by the authors [5] discussed one way to simplify a feedback controller, by reducing the number of actuators and sensors needed for good performance. The work was done on a tensioned aircraft-style panel excited on one side by TBL flow in a low speed wind tunnel. Actuation was provided by a piezoelectric (PZT) actuator mounted on the center of the panel. For sensing, the responses of four accelerometers, positioned to approximate the response of the first radiation mode of the panel, were summed and fed back through the controller. This single input-single output topology was found to have nearly the same noise reduction performance as a controller with fifteen accelerometers and three PZT patches.

This paper extends the previous results by looking at how constrained layer damping (CLD) on a panel can be used to enhance the performance of the feedback controller thus providing a more robust and efficient hybrid active/passive system. The eventual goal is to use the CLD to reduce sound radiation at high frequencies, then implement a very simple, reduced order, low sample rate adaptive controller to attenuate sound radiation at low frequencies. Additionally this added damping smoothes phase transitions over the bandwidth which promotes robustness to natural frequency shifts.

Experiments were conducted in a transmission loss facility on a clamped-clamped aluminum panel driven on one side by a loudspeaker. A generalized predictive control (GPC) algorithm, which is suited to online adaptation of its parameters [6], was used in single input-single output and multiple input-single output configurations. Because this was a preliminary look at the potential of constrained layer damping for adaptive control, static feedback control with no online adaptation was used. Two configurations of CLD in addition to a bare panel configuration were studied. For each CLD configuration, two sensor arrangements for the feedback controller were compared. The first arrangement used fifteen accelerometers on the panel to estimate the responses of the first six radiation modes of the panel [7]. The second sensor arrangement was simpler, using the summed responses of only four accelerometers to approximate the response of the first radiation mode of the panel. In all cases a PZT patch was mounted at the center of the panel for control input. The performance of the controller was quantified using the responses of the fifteen accelerometers on the panel to estimate radiated sound power. The paper begins with a brief discussion of the GPC algorithm and the experimental setup. The experimental results are discussed next, comparing the CLD and sensor configurations, followed by discussion and conclusions.

ANALYSIS

Control Algorithm. The controls approach used here is similar to that described by Baumann [8] and elaborated on by others [7, 9]. The general philosophy is to formulate the control of structural radiation as an optimal control problem. An important aspect of the formulation is the use of structural sensors, such as accelerometers, whose responses are processed through a radiation filter matrix to derive time domain responses of a set of radiation modes. The time averaged, squared amplitudes of the radiation mode responses are related to total radiated acoustic power [9]. To compute the radiation modal responses accurately requires a large number of structural sensors, so an approach using fewer sensors is studied here as well. The simplified sensor topology is used to estimate sound radiation due to volumetric motion, which has been found to be useful for reducing sound radiation from a panel [5, 10].

One cost function for the optimal control problem corresponds to that of the linear quadratic regulator (LQR) [11], written

$$J = \int_0^\infty \left(\mathbf{z}^T \mathbf{z} + \lambda \mathbf{u}^T \mathbf{u} \right) \tag{1}$$

where $\mathbf{z}$ denotes a vector of measured or derived system responses, $\mathbf{u}$ denotes a vector of actuator inputs, and λ regulates the control effort used in the optimal solution. An example of derived responses would be the radiation mode responses which are computed from the accelerometer responses. A more attractive controls approach for the adaptive problem, where the control input may have to be updated online in a recursive fashion, is generalized predictive control [6, 11]. The cost function for a generalized predictive controller is similar to Eq. 1, but the time horizon is finite, rather than infinite, and is written [12]

$$J = \sum_{i=0}^{p-1} ||\mathbf{z}(k+i)||^2 + \lambda ||\mathbf{u}(k+i)||^2 \tag{2}$$

where k denotes the current time index, and p defines the time horizon over which the cost function is defined. Because the time horizon is finite, computation of the optimal control input is much simpler than for an LQR controller [11]. For a time invariant plant, which was assumed in the current experiment, the optimal controller is also time invariant. With this assumption, the optimal controller is computed once at the start of an experiment and not updated while the controller is running.

The solution of the optimal controller defined by Eq. 2 requires a model of the path from the control input, $\mathbf{u}$, to the system responses, $\mathbf{z}$. For controlling sound radiation, the system responses consisted of accelerometer responses transformed through a radiation filter matrix [8]. Because this transformation can be computationally intensive, the radiation modal expansion technique, which uses a reduced order model of the radiation filter matrix, was used to simplify the real-time controller implementation [5, 7, 13]. The time domain outputs of the radiation filter matrix were the responses of the radiation modes of the structure, and these responses made up the elements of the $\mathbf{z}$ vector in the cost function. As mentioned previously, two sensor arrangements were used in this experiment. For the first arrangement, the responses of fifteen accelerometers uniformly arranged on the panel were used to estimate the responses of
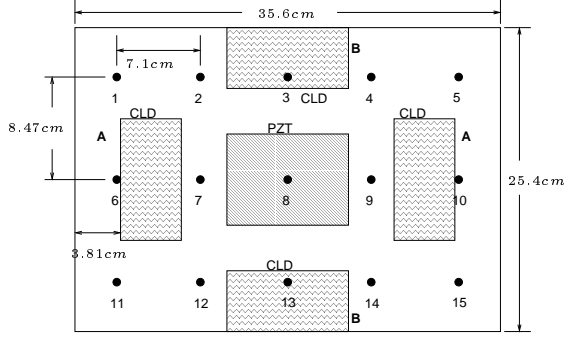
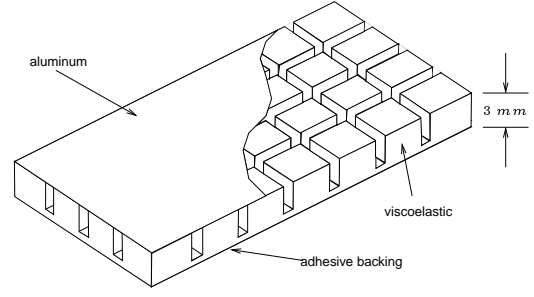Figure 1: Accelerometers, PZT and CLD on panel

Figure 2: Cut-away of CLD

the first six radiation modes of the structure. For the second sensor arrangement, the time domain responses of four accelerometers were summed to create a single signal which was a crude approximation to the response of the first radiation mode of the structure [5]. By summing the accelerometer responses, the contributions of inefficiently radiating panel modes were minimized. Both configurations were based on the concept of elemental radiators described in reference [14].

A time domain system identification technique [15] was used to model the plant from actuator input to either the radiation mode responses or the summed accelerometer response. The plant was excited by the PZT driven with white noise shaped with a low pass filter to enhance excitation at low frequencies. For the radiation mode response configuration, a single input, six output state space model with 84 states was computed along with an optimal state observer. Control was implemented using full state feedback, so the control input to the PZT at time (k) was computed as $u(k) = -\mathbf{K}\mathbf{x}(k)$, where $\mathbf{x}$ denotes the state vector and $\mathbf{K}$ is the feedback gain matrix computed by solving the controller cost function, Eq. 2. For the simpler sensor configuration, the system was modeled using an auto-regressive moving average with exogenous input (ARX) model. The control input for this case was computed as a weighted sum of past inputs and outputs,

$$u(k) = \sum_{i=1}^{p} \left(G_i u(k - i) + H_i z(k - i) \right) \tag{3}$$

where $p = 100$. This representation is especially suitable for online adaptation of the controller parameters [12].

Facility. Testing was done on a $254mm \times 356mm \times 1mm$ thick aluminum panel clamped on all sides and mounted in a transmission loss facility. The panel is shown in the schematic in Fig. 1. The dynamics of this panel are simpler than an actual aircraft panel, and the damping is also lower, but the structure was still useful for studying the influence of constrained layer damping on a feedback controller. A disturbance excitation was produced by a loudspeaker in the source room driven with an 800 Hz bandwidth random signal. Control actuation was provided with two PZT actuators, each measuring $110mm \times 38mm \times 0.76mm$, mounted on the center of the source room side of the panel. The actuator inputs were wired together, and so they appeared to the control system as a single actuator. Fifteen accelerometers, denoted by the numbered circles in Fig. 1, were mounted on the receiver room side of the panel. All fifteen accelerometers were used for the radiation mode controller, and accelerometers 3, 7, 9, and 13 were used for the simpler four-accelerometer controller. Note that summing the time domain responses of these four accelerometers filters out the contributions of low order even modes, which are inefficient radiators of sound.

Two configurations of constrained layer damping (CLD), henceforth referred to as the A and B configurations, were tested. The CLD material, shown in a cut-away view in Fig. 2, was $3\ mm$ thick, weighed $2.07\ kg/m^2$, and had regularly spaced grooves cut into the viscoelastic material. Each configuration consisted of three strips of CLD, with dimensions $50.8mm \times 101.6mm$, on the source room side of the panel. The strips weighed a total of 30.2 g, or 12.6% of the mass of the bare panel, and covered 17.1% of the total panel area. For both configurations, one strip of CLD, not shown in Fig. 2, was placed on top of the PZT which is a high strain location for the odd-odd panel modes. The other two strips were placed in either the A or Blocations in Fig. 2. These locations were chosen with some consideration of the curvature of panel modes that contributed significantly to sound radiation, but the locations were not optimized in

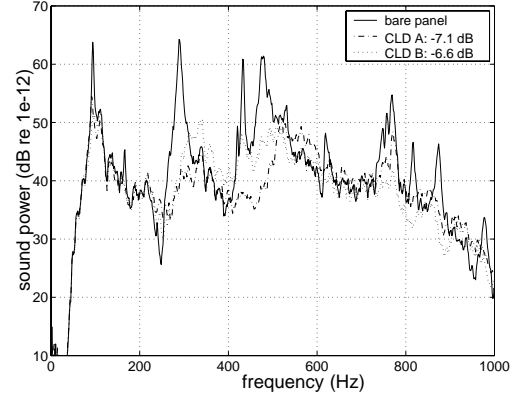| Mode	Damping (%)		
(horiz., vert.)	bare panel	A	B
(1,1)	1.6	2.7	4.3
(3,1)	0.8	6.4	4.1
(1,3)	1.1	5.4	4.6

Table 1: Modal damping percentages

Figure 3: Performance of CLD

a formal sense. The A locations were chosen so as to add damping to the (4,1) panel mode, which was not controllable by the PZT, and the (2,3) and (5,2) panel modes. The B locations were chosen to add damping to the (1,1) and (3,1) modes, in addition to the damping provided by the center strip of CLD.

Control and data acquisition were handled by a PC-based system using TMS320C40 digital signal processors (DSP). The controller operated at 2000 Hz with anti-aliasing and reconstruction filters set to 800 Hz. Controller performance was monitored using the 15 accelerometers sampled with a separate DSP system running at 5000 Hz.

RESULTS

The passive damping provided by the constrained layer damping will be presented first, followed by closed loop results for the two feedback sensor arrangements. In all cases, the controller performance is quantified in terms of reductions in radiated sound power using the elemental radiator approach [14] and the responses of the 15 accelerometers on the panel.

The passive damping provided by the CLD is summarized in terms of modal damping percentages in Table 1 and radiated sound power in Fig. 3. The percentages in Table 1 indicate that both CLD configurations added significant damping to the odd-odd panel modes. In terms of radiated sound power integrated from 50 to 800 Hz, the reduction was 7.1 dB for CLD at the A locations and 6.6 dB for CLD in the B locations. Both CLD configurations had a similar effect on the (1,1) mode: Integrated from 70 to 125 Hz, the radiated sound power was reduced by 5.2 dB and 5.7 dB for A and B, respectively. From 400 to 600 Hz, which contains the natural frequencies of the (4,1) and (1,3) modes, the integrated reduction for A was 7.5 dB and for B was 7.0 dB. In spite of the similar reductions, the damping provided by the CLD between 400 and 600 Hz was very location dependent, with the A configuration adding significantly more damping to the (4,1) mode just above 400 Hz.

Closed loop results for controlling responses of the first six radiation modes of the panel are shown in Fig. 4. The closed loop reduction in radiated sound power integrated from 50 to 800 Hz was 5.3 dB for the bare panel, 9.2 dB for the A CLD configuration, and 7.7 dB for B. Relative to the passively damped configurations with CLD only, the feedback controller produced additional reductions over the entire bandwidth of 2.1 dB for A and 1.1 dB for B. Although not readily visible in the figure, the (4,1) mode at 420 Hz and the (5,2) mode near 750 Hz were not controllable, so the bare panel results overlay the open loop results at those frequencies. Between 70 and 125 Hz, the B configuration performed slightly better than A with a reduction of 8.9 dB to A's 7.8 dB. From 400 to 600 Hz, the A configuration reduced the radiated sound power by 10.1 dB, whereas the B configuration reduced it by only 7.5 dB. The difference appears to be due to reductions obtained at the (4,1) mode near 420 Hz.

The closed loop results for the simpler control configuration using only four accelerometers are shown in Fig 5. The bare panel results are not nearly as good as the bare panel results for the radiation mode controller. However, the reductions obtained with CLD in either configuration are relatively close to those obtained with the radiation mode controller. Integrated from 50 to 800 Hz, the reductions obtained were 3.0 dB for no CLD, 8.8 dB for the A CLD configuration, and 7.0 dB for the B configuration. Although not shown here, the controller in the bare panel
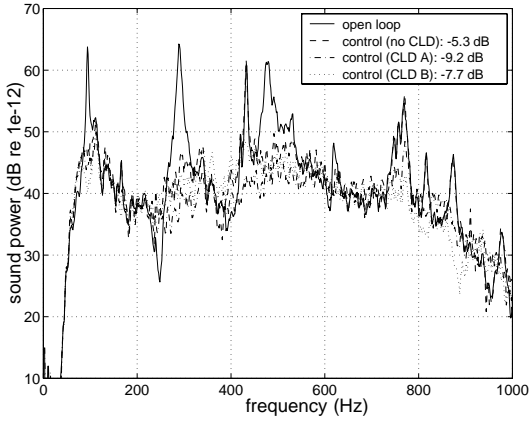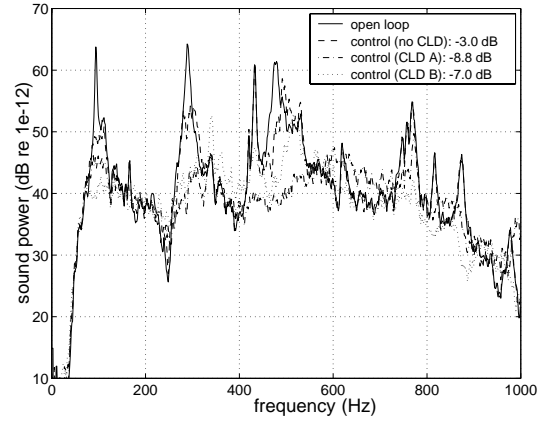
Figure 4: Radiation mode control

Figure 5: Diamond accelerometer control

case produced significant reductions in the controller cost function, which was the sum of the responses of the four accelerometers. This performance did not translate into significant reductions in radiated sound power. However, with CLD on the panel, reductions in the summed accelerometer responses did produce reductions in radiated sound power. A likely reason for this behavior is that the feedback controller was less aggressive when CLD was on the panel due to the significant amount of passive damping provided by the CLD. Because the controller was less aggressive, it was less likely to drive the panel in such a way as to increase radiated sound power.

The simple controller was able to surpass the performance of the more complicated radiation mode controller in certain areas of the spectrum. The reduction integrated from 70 to 125 Hz was 9.7 dB and 13.1 dB for the A and B cases, respectively, both of which are greater than the reductions obtained with the radiation mode controller over that same bandwidth. From 400 to 600 Hz, the integrated reduction was 10.8 dB for the A configuration and 6.3 dB for the B configuration, which are, respectively, 0.7 dB more and 1.2 dB less than the radiation mode controller. The good performance of the simple controller was possible because the sound radiation from this panel in this frequency range was dominated by the first radiation mode of the structure. When the simple four accelerometer cost function provided a good approximation to the response of the first radiation mode, the simple controller performed well. This was most apparent for the A CLD configuration, because the simple cost function for this configuration closely matched the response of the first radiation mode near the (1,1) and (1,3) panel modes. The match was not as close for the B configuration, which could have been a result of a slight change in the boundary conditions due to the B CLD locations.

The closed loop performance of the simple controller with the A configuration is a promising start for simplifying the feedback controller with CLD. However, the sensitivity of performance to CLD location indicates that optimization of the CLD placement together with the controller cost function is a difficult problem that is tightly coupled with the disturbance spectrum and panel dynamics in the bandwidth of interest.

CONCLUSIONS

The hybrid active/passive control results described here illustrate how constrained layer damping (CLD) can help a simple feedback controller topology produce reductions in radiated sound power that are close to those of a much more complicated controller topology. In this simple experiment, a single input/single output controller, with CLD on the panel, reduced the sound power transmitted through a clamped panel by 8.8 dB integrated from 50 to 800 Hz. In comparison, a more complicated controller that required fifteen accelerometers whose outputs were processed to compute radiation mode responses, reduced the sound power by 9.2 dB.

The results also illustrate that the impact of the CLD on the closed loop performance depends on the CLD's placement on the structure and on the control cost function. With CLD on the center and sides of the panel (the A configuration), sound radiated near the natural frequency of the (1,1) panel mode was reduced by 7.8 dB for the radiation mode cost function, and by 9.7 dB for the simpler four accelerometer cost function. With CLD on the top, center, and bottom of the panel, the reduction at the (1,1) panel mode was 8.9 dB for the radiation mode controller but

13.1 dB for the simpler controller.

The results demonstrate that for this very simple system there is considerable benefit to designing the passive and active characteristics of the controller together. Careful optimization of the CLD placement and controller cost function could be used to implement a low bandwidth, reduced order feedback controller which would be amenable to online adaptation of the controller parameters. Considerable work remains to be done in order to apply this approach to the much more complicated dynamics of a real aircraft panel subject to varying flight conditions.

REFERENCES

[1] D.E. Cox, G.P. Gibbs, R.L. Clark, and J.S. Vipperman. Experimental robust control of structural acoustic radiation. *ASME Journal of Vibration and Acoustics*, 121:433–439, 1999.

[2] Stephen J. Elliott and Trevor J. Sutton. Performance of feedforward and feedback systems for active control. *IEEE Transactions on Speech, and Audio Processing*, 4(3):214–223, May 1996.

[3] Kemin Zhou, John C. Doyle, and Keith Glover. *Robust and Optimal Control*. Prentice Hall, 1996.

[4] Karl J. Åström and Björn Wittenmark. *Adaptive Control*. Addison Wesley, 2nd edition, 1995.

[5] G.P. Gibbs, R.H. Cabell, and J. Juang. Controller complexity for active control of TBL induced sound radiation from panels. In *6th AIAA/CEAS Aeroacoustics Conference*, number AIAA 2000-2043, Lahaina, Hawaii, June 12-14 2000.

[6] D.W. Clarke, C. Mohtadi, and P.S. Tuffs. Generalized predictive control - Part I. The basic algorithm. *Automatica*, 23(2):137–148, 1987.

[7] Gary P. Gibbs, Robert L. Clark, David E. Cox, and Jeffrey S. Vipperman. Radiation modal expansion: Application to active structural acoustic control. *Journal of the Acoustical Society of America*, 107(1):332–339, January 2000.

[8] William T. Baumann, William R. Saunders, and Harry H. Robertshaw. Active suppression of acoustic radiation from impulsively excited structures. *Journal of the Acoustical Society of America*, 90(6):3202–3208, December 1991.

[9] D.R. Thomas and P.A. Nelson. Feedback control of sound radiation from a plate excited by a turbulent boundary layer. *Journal of the Acoustical Society of America*, 98(5):2651–2662, November 1995.

[10] M.E. Johnson and S.J. Elliott. Active control of sound radiation using volume veclocity cancellation. *Journal of the Acoustical Society of America*, 98(4):2174–2186, 1995.

[11] Edoardo Mosca. *Optimal, Predictive, and Adaptive Control*. Prentice Hall, 1995.

[12] Jer-Nan Juang and Minh Phan. Deadbeat predictive controllers. Technical Report TM-112862, NASA Langley Research Center, May 1997.

[13] Gary P. Gibbs, Kenneth W. Eure, and John W. Lloyd. Active control of turbulent boundary layer induced sound radiation from aircraft style panels. In *Proceedings of Active-99*, Ft. Lauderdale, Florida, December 1999.

[14] S. J. Elliott and M. E. Johnson. Radiation modes and the active control of sound power. *Journal of the Acoustical Society of America*, 94(4):2194–2204, October 1993.

[15] J. Juang, L.G. Horta, and M. Phan. System/observer/controller identification toolbox. Technical Report TM-107566, NASA Langley Research Center, 1992.